Measurement of the Decay $K_L \to \pi^0 e^+ e^- \gamma$

E. Abouzaid,[4] M. Arenton,[11] A.R. Barker,[5, *] L. Bellantoni,[7] E. Blucher,[4] G.J. Bock,[7] E. Cheu,[1] R. Coleman,[7] B. Cox,[11] A.R. Erwin,[12] C.O. Escobar,[3] A. Glazov,[4] A. Golossanov,[11] R.A. Gomes,[3] P. Gouffon,[10] Y.B. Hsiung,[7] D.A. Jensen,[7] R. Kessler,[4] Y.J. Kim,[1] K. Kotera,[8] A. Ledovskoy,[11] P.L. McBride,[7] E. Monnier,[4, †] K.S. Nelson,[11] H. Nguyen,[7] R. Niclasen,[5] D.G. Phillips II,[11] H. Ping,[12] E.J. Ramberg,[7] R.E. Ray,[7] M. Ronquest,[11] E. Santos,[10] W. Slater,[2] D. Smith,[11] N. Solomey,[4] E.C. Swallow,[4, 6] P.A. Toale,[5] R. Tschirhart,[7] C. Velissaris,[12] Y.W. Wah,[4] J. Wang,[1] H.B. White,[7] J. Whitmore,[7] M. J. Wilking,[5] B. Winstein,[4] R. Winston,[4] E.T. Worcester,[4] M. Worcester,[4] T. Yamanaka,[8] E. D. Zimmerman,[5] and R.F. Zukanovich[10]

[1] *University of Arizona, Tucson, Arizona 85721*
[2] *University of California at Los Angeles, Los Angeles, California 90095*
[3] *Universidade Estadual de Campinas, Campinas, Brazil 13083-970*
[4] *The Enrico Fermi Institute, The University of Chicago, Chicago, Illinois 60637*
[5] *University of Colorado, Boulder, Colorado 80309*
[6] *Elmhurst College, Elmhurst, Illinois 60126*
[7] *Fermi National Accelerator Laboratory, Batavia, Illinois 60510*
[8] *Osaka University, Toyonaka, Osaka 560-0043 Japan*
[9] *Rice University, Houston, Texas 77005*
[10] *Universidade de São Paulo, São Paulo, Brazil 05315-970*
[11] *The Department of Physics and Institute of Nuclear and Particle Physics, University of Virginia, Charlottesville, Virginia 22901*
[12] *University of Wisconsin, Madison, Wisconsin 53706*
(Dated: June 13, 2007)

We report on a new measurement of the branching ratio BR($K_L \to \pi^0 e^+ e^- \gamma$) using the KTeV detector. This analysis uses the full KTeV data set collected from 1997 to 2000. We reconstruct 139 events over a background of 14, which results in BR($K_L \to \pi^0 e^+ e^- \gamma$) = $(1.62 \pm 0.14_{stat} \pm 0.09_{syst}) \times 10^{-8}$. This result supercedes the earlier KTeV measurement of this branching ratio.

PACS numbers: 13.20.Eb, 11.30.Er, 12.39.Fe, 13.40.Gp

I. INTRODUCTION

The decay $K_L \to \pi^0 e^+ e^- \gamma$ can be used to study the low-energy dynamics of neutral K mesons. In particular, this decay is an important check of Chiral Perturbation Theory (ChPT), which has been used to describe kaon decays in which long distance effects dominate. Up to $O(p^4)$ in chiral perturbation theory, there are no free parameters and one predicts the branching ratio to be approximately 1.0×10^{-8}[1]. In the related decay $K_L \to \pi^0 \gamma\gamma$, the $O(p^4)$ calculation was found to underestimate the measured branching ratio by a factor of three[2–6]. To match the data it was found necessary to extend the calculation to include $O(p^6)$ terms while introducing vector meson exchange terms[7]. The addition of both of these effects into the $K_L \to \pi^0 e^+ e^- \gamma$ calculation results in an increase in the branching ratio to 2.4×10^{-8}, approximately twice the $O(p^4)$ calculation. Two previous experimental results have been reported on this decay mode[8–10]. The most recent measurement comes from the KTeV 1997 data set and is based on 48 events with a background of 3.6±1.1 events. That measurement yielded BR($K_L \to \pi^0 e^+ e^- \gamma$) = $(2.34 \pm 0.35 \pm 0.13) \times 10^{-8}$,

but must be rescaled to $(2.17 \pm 0.32 \pm 0.12) \times 10^{-8}$ when using the latest measurement of BR($K_L \to \pi^0 \pi^0$)[11, 12]. For this analysis, we use improved techniques to reanalyze the 1997 data set and combine it with a new measurement from the 1999 data set.

The $K_L \to \pi^0 e^+ e^- \gamma$ decay can also be used to help understand the CP violating decay, $K_L \to \pi^0 e^+ e^-$. The $K_L \to \pi^0 e^+ e^-$ decay contains both CP violating and CP conserving amplitudes. Since the $K_L \to \pi^0 e^+ e^- \gamma$ decay proceeds through a two photon intermediate state, it can be used to determine the CP conserving components in $K_L \to \pi^0 e^+ e^-$, and thus allow one to determine the CP violating contribution in $K_L \to \pi^0 e^+ e^-$. Also, because the rate for $K_L \to \pi^0 e^+ e^- \gamma$ is orders of magnitude higher than the rate for $K_L \to \pi^0 e^+ e^-$, this decay can act as a source of background in the search for $K_L \to \pi^0 e^+ e^-$.

II. THE KTEV DETECTOR

We collect $K_L \to \pi^0 e^+ e^- \gamma$ events using the KTeV detector located at Fermilab. The data analyzed were taken during the 1997 and 1999 rare decay running periods and comprised 2.9×10^{11} and 3.8×10^{11} kaon decays, respectively. The KTeV experiment employed two different configurations during its operation. The E799 configuration was used for this measurement and was optimized for reconstructing rare kaon decays.
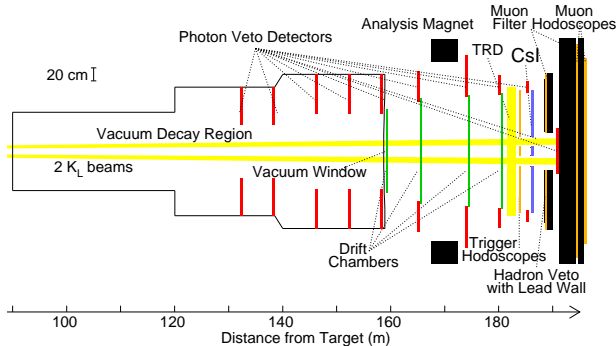
FIG. 1: Schematic of the KTeV detector.

In the KTeV experiment[13] neutral kaons are produced in interactions of 800 GeV/c protons with a beryllium oxide target. The resulting particles pass through a series of collimators to produce two nearly parallel beams. The beams also pass through lead and beryllium absorbers to reduce the fraction of photons and neutrons in each beam. Charged particles are removed from the beams by sweeping magnets located downstream of the collimators. The vacuum decay volume begins approximately 94 meters downstream of the target, far enough so that the majority of the K_S mesons have decayed, and extends to approximately 159 meters from the target. The decay volume is surrounded by photon veto detectors that reject photons at angles greater than 100 milliradians.

The most critical detector elements for this analysis are a charged particle spectrometer and a pure CsI electromagnetic calorimeter[14]. The KTeV spectrometer is used for reconstructing charged tracks. This spectrometer consists of four planes of drift chambers; two located upstream and two downstream of an analyzing magnet with a transverse momentum kick of 0.205 GeV/c. Each drift chamber contains four planes of wires; two to measure the horizontal position and two to measure the vertical position with a precision of approximately 100μm. During data taking in 1999 the momentum kick was reduced to 0.150 GeV/c to increase the acceptance for multi-track events.

The CsI calorimeter is composed of 3100 blocks in a 1.9 m by 1.9 m array. The depth of the CsI calorimeter corresponds to 27 radiation lengths. Two 15 cm by 15 cm holes are located near the center of the array for the passage of the two neutral beams. For electrons with energies between 2 and 60 GeV, the calorimeter energy resolution is below 1% and the nonlinearity is less than 0.5%. The position resolution of the calorimeter is approximately 1 mm. Downstream of the CsI calorimeter, there is a 10 cm lead wall, followed by a hodoscope used to reject hadrons hitting the calorimeter.

The $K_L \rightarrow \pi^0 e^+ e^- \gamma$ decays were required to satisfy certain trigger requirements in order to be recorded. In particular, activity in a set of hodoscopes upstream of the CsI calorimeter had to be consistent with two tracks. Also, we required the event have at least one hit in one of the two upstream drift chambers. The event must deposit more than approximately 25 GeV of total energy in the CsI calorimeter and no more than 0.5 GeV in the photon vetoes. The event is vetoed if it deposits more than 2.5 Mips in the hodoscope downstream of the calorimeter or more than 14 GeV in the vetoes around the beam holes in the CsI calorimeter. The trigger includes a hardware cluster processor that counts the number of in-time calorimeter clusters of contiguous blocks of CsI with energies above 1 GeV[15]. The total number of electromagnetic clusters in the CsI calorimeter is required to be greater than or equal to four at the trigger level.

After the events are read out, they must satisfy a software filter. This filter requires that each event have two charged tracks with a minimum of four clusters in the calorimeter. Each of the tracks must point to a cluster in the calorimeter and be consistent with an electron hypothesis. The trigger requirements also select $K_L \rightarrow \pi^0 \pi_D^0$ events where the neutral pion undergoes Dalitz decay, $\pi^0 \rightarrow e^+ e^- \gamma$ (π_D^0). These events are used for normalizing the $K_L \rightarrow \pi^0 e^+ e^- \gamma$ events, since their topology is very similar to that of our signal events. Because of the similarity in topologies between the signal and normalization modes, many systematic effects cancel.

III.   EVENT RECONSTRUCTION

The offline analysis begins by requiring that each event have exactly two oppositely signed tracks and five in-time clusters with energies greater than 2.0 GeV, where an in-time cluster is one in which the cluster reconstructs to within 19 ns of the event time. The two tracks are required to point to two of the clusters and be consistent with a common decay vertex. From the three neutral clusters, we combine two to form the π^0 candidate. There are three possible combinations and we choose the combination that reconstructs closest to the π^0 mass. Only events with a $\gamma\gamma$ invariant mass within 5 MeV/c^2 of the nominal π^0 mass are accepted. The neutral decay distance vertex is used to determine the mass of the $e^+ e^- \gamma$ and $e^+ e^- \gamma\gamma\gamma$ combinations because it improves their mass resolution; the $e^+ e^-$ tracks tend to be close together leading to poorer vertex resolution. The total kaon energy, determined from the sum of cluster energies in the calorimeter, must lie between 30 and 210 GeV.

To ensure that the two tracks are electrons, the reconstructed energy in the calorimeter divided by the momentum determined by the spectrometer (E/p) of each track must be between 0.95 and 1.05. Backgrounds from K_s decays and misreconstructed kaons can be reduced by requiring the decay vertex to reconstruct between 98 and 157 meters downstream of the target, and the transverse momentum squared (p_T^2) for the event to be less than
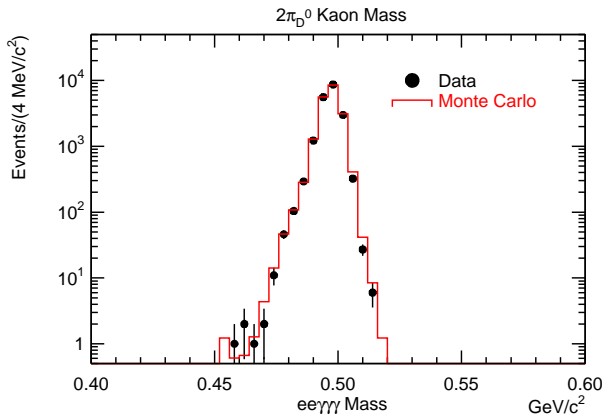
FIG. 2: The $K_L \to \pi^0 \pi_D^0$ invariant mass distribution for data (dots) and $K_L \to \pi^0 \pi_D^0$ Monte Carlo (solid histogram).

0.003 $(\text{GeV}/c)^2$. The invariant mass for $K_L \to \pi^0 \pi_D^0$ events is shown in Figure 2. The data and our Monte Carlo simulation agree quite well.

IV. BACKGROUNDS TO $K_L \to \pi^0 e^+ e^- \gamma$

After applying the above selection criteria, the remaining backgrounds consist mainly of $K_L \to \pi^0 \pi_D^0$ and $K_L \to \pi^0 \pi^0 \pi_D^0$ decays. The $K_L \to \pi^0 \pi_D^0$ decays are more readily removed because the invariant masses of the $e^+ e^- \gamma$ and $\gamma\gamma$ combinations reconstruct around the mass of the π^0. However, when the wrong $\gamma\gamma$ combination is chosen, a restriction on the invariant masses is ineffective at reducing the background. $K_L \to \pi^0 \pi_D^0$ events can also contribute to the background if one of the final state particles is lost and is replaced by an accidental particle. Accidental particles result from activity in the detector that can mimic a final state particle. The $K_L \to \pi^0 \pi^0 \pi_D^0$ events are more difficult to remove because we cannot use the same mass constraints as in the $K_L \to \pi^0 \pi_D^0$ case. However, kinematic and cluster shape variables have been developed to help to reduce the background to a manageable level.

To remove misreconstructed $K_L \to \pi^0 \pi_D^0$ decays, we consider the two other possible $\gamma\gamma$ combinations. We take advantage of the correlations between the $m_{\gamma\gamma}$ and $m_{e^+ e^- \gamma}$ distributions for these two combinations, forming a neural net from four variables. These four input variables are the reconstructed invariant $\gamma\gamma$ and $e^+ e^- \gamma$ masses for each of the two remaining combinations. The neural net employed sixteen hidden nodes and was tuned on a sample of $2\pi_D^0$ and $\pi^0 e^+ e^- \gamma$ Monte Carlo. The output from the neural net ranges between zero and one. We rejected events where the neural net value was less than 0.5.

Backgrounds from $K_L \to \pi^0 \pi^0 \pi_D^0$ come from two broad classes of events: events with missing photons and those with one or more photons that overlap or fuse to-
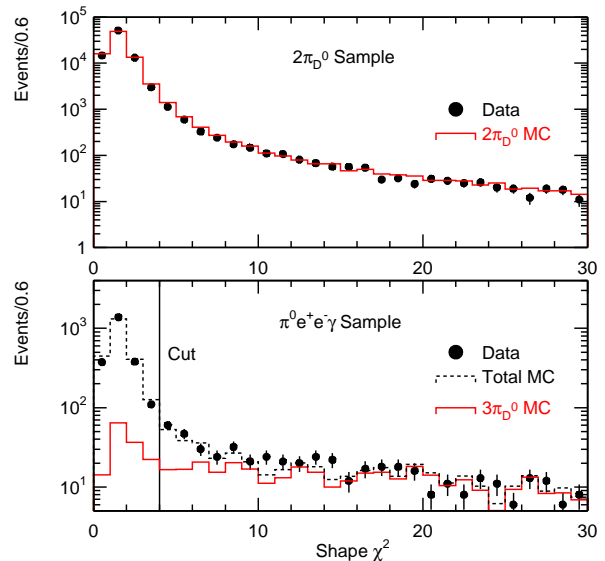
FIG. 3: The photon shape variable shape χ^2. The top plot shows the shape χ^2 variable for $K_L \to \pi^0 \pi_D^0$ with the dots representing the data and the solid histogram the Monte Carlo. In the bottom histogram the dots are the data after removing the $K_L \to \pi^0 \pi_D^0$ events, while the solid histogram shows the $K_L \to \pi^0 \pi^0 \pi_D^0$ Monte Carlo. The dashed histogram represents the sum of the signal and background Monte Carlo samples.

gether in the CsI calorimeter. For events with missing photons, we use the photon vetoes to significantly reduce the amount of background. We require the maximum energy in any photon veto to be less than 0.1 GeV. To reduce backgrounds from events with overlapping photons, we examined the calorimeter energies in a 3×3 array of crystals centered around the highest energy crystal of the cluster. For reference, the Molière radius in CsI is 3.8 cm. We compared these energies to energies from an ideal cluster shape and calculated a photon shape χ^2 variable. This variable is shown in Figure 3. As can be seen, for the normalization mode, there is good agreement in this variable between the data and the Monte Carlo simulation. For the signal events, the background from $K_L \to \pi^0 \pi^0 \pi_D^0$ events is significantly reduced by requiring a small value of shape χ^2. We require shape χ^2 < 4.

Kaon decays with missing photons will also exhibit a significant amount of missing energy when boosted to the center-of-mass. We take advantage of this effect by calculating the longitudinal missing momentum in the center-of-mass (pp0kine). In the pp0kine versus $m_{\gamma\gamma\gamma}$ plane, the signal events are well-separated from the $K_L \to \pi^0 \pi^0 \pi_D^0$ background. We define a two dimensional cut by employing the following fourth-order polynomial:

$$
\begin{aligned}
\text{pp0kine}_{max} = \; & A + B * (m_{\gamma\gamma\gamma} - x_0) + C * (m_{\gamma\gamma\gamma} - x_0)^2 \\
& + D * (m_{\gamma\gamma\gamma} - x_0)^3 + E * (m_{\gamma\gamma\gamma} - x_0)^4.
\end{aligned}
$$
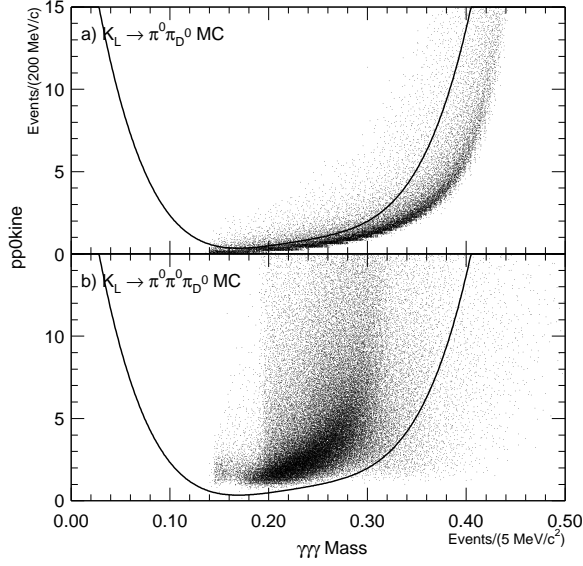
FIG. 4: The pp0kine variable plotted versus the $\gamma\gamma\gamma$ invariant mass for a) $K_L \to \pi^0\pi_D^0$ and b) $K_L \to \pi^0\pi^0\pi_D^0$ Monte Carlo events. The dark line represents the cut indicated in the text.

where A = 3.9, B=-112.8, C=1256.6, D=-5861.8, E=10506.0 and $x_0 = 8.326 \times 10^{-2}$. The values of these parameters were chosen to maximize the signl-to-background ratio. Events with values of pp0kine greater than this value were rejected. This cut is shown in Fig. 4.

V. RESULTS

After making these final selection criteria, we find the $e^+e^-\gamma\gamma\gamma$ mass distributions shown in Figure 5. A clear peak at the kaon mass is seen, while the background is well-described by the sum of the $2\pi_D^0$ and $3\pi_D^0$ background Monte Carlo samples. We find a total of 139 candidate events with an estimated background of 14.4 ± 2.5 events.

The $K_L \to \pi^0 e^+ e^- \gamma$ branching fraction is determined from the following expression:

$$
\begin{aligned}
BR = & (N_{\pi^0 e^+ e^- \gamma}/N_{2\pi^0}) \times (\epsilon_{2\pi^0}/\epsilon_{\pi^0 e^+ e^- \gamma}) \\
& \times BR(K_L \to \pi^0\pi^0) \times BR(\pi^0 \to e^+e^-\gamma) \times 2.
\end{aligned}
$$

Here, $N_{\pi^0 e^+ e^- \gamma}$ represents the number of signal candidates, while $N_{2\pi^0}$ represents the number of normalization events. The number of $K_L \to \pi^0\pi_D^0$ candidates is determined by removing the cut against $K_L \to \pi^0\pi_D^0$ events and counting the number of events in the kaon mass region from 0.490 to 0.510. In the above expression $\epsilon_{2\pi^0}$ and $\epsilon_{\pi^0 e^+ e^- \gamma}$ correspond to the reconstructed $K_L \to 2\pi^0$ and $K_L \to \pi^0 e^+ e^- \gamma$ acceptances, respectively. The factor of two occurs because there are two π^0 in each $K_L \to \pi^0\pi_D^0$ event. In the previous analysis, the value of $BR(K_L \to \pi^0\pi^0)$ used was $(9.36 \pm 0.2) \times 10^{-4}$. We are now using the most recent
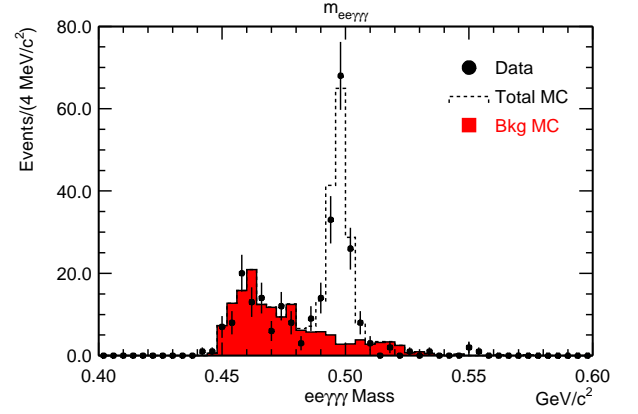
FIG. 5: The $e^+e^-\gamma\gamma\gamma$ invariant mass for events passing all selection criteria. The dots represent the data, while the dashed histogram represents the sum of the signal and background Monte Carlo. The background Monte Carlo is indicated by the shaded histogram.

determination of $BR(K_L \to \pi^0\pi^0) = (8.69 \pm 0.08) \times 10^{-4}$. The value of $BR(\pi^0 \to e^+e^-\gamma)$ used in both analyses is $(1.198 \pm 0.032) \times 10^{-2}$.

The acceptance for $K_L \to 2\pi_D^0$ events is 0.51% in the 1997 data set and 0.61% in the 1999 data set. The difference between the acceptances in the two data sets arises from the different magnetic fields used during the 1997 and 1999 runs. We find 31,286 $K_L \to \pi^0\pi_D^0$ events in the 1997 data and 49,159 events in the 1999 data. This corresponds to a kaon flux of 2.88×10^{11} and 3.78×10^{11} decays in the 1997 and 1999 data sets, respectively. The $\pi^0 e^+ e^- \gamma$ acceptances are 0.90% and 1.02% for the 1997 and 1999 data sets, respectively. These values are shown in Table I. Using the numbers above, we obtain:

$$
\begin{aligned}
BR(K_L \to \pi^0 e^+ e^- \gamma) &= (1.49 \pm 0.22) \times 10^{-8} \quad (1997) \\
BR(K_L \to \pi^0 e^+ e^- \gamma) &= (1.77 \pm 0.18) \times 10^{-8} \quad (1999)
\end{aligned}
$$

The branching ratio for the 1997 data is consistent with the published 1997 value after correcting the published value for the updated $K_L \to \pi^0\pi^0$ branching ratio and the difference in acceptance due to more recent measurements of a_V[6].

Value	1997	1999
Events in Data	47	92
Background Events	2.7	11.7
Normalization Events	31,286	49,159
Signal Acceptance	0.91%	1.03%
Normalization Acceptance	0.51%	0.61%

TABLE I: Values used in branching ratio calculation.